# IRANIAN JOURNAL OF CATALYSIS

# Investigation efficiency of nano photocatalytic compound of TiO$_2$ and rice husk silica in removal of reactive red 198 dye from synthetic aqueous solutions

**Abdollrahman Mahmoodi[a], Seyed Mahmood Mehdinia[b], Ayat Rahmani[a], Hamidreza Nassehinia[a],***

*[a]Department of Environmental Health Engineering, Semnan University of Medical Sciences, Semnan, Iran.*
*[b]Department of Environmental Health Engineering, Babol University of Medical Sciences, Babol, Iran.*

## ABSTRACT

This study was performed with the aim of investigating the efficiency of the Nano photocatalytic of ultraviolet and titanium dioxide compound and rice husk silica adsorbent (UV/TiO$_2$/RHS) in removal reactive red 198 dye from synthetic aqueous solutions. The removal of reactive red 198 dye was done in batch reactors with a volume of 250 ml using RHS deposited by titanium dioxide in the presence of a UV lamp. The effect of pH, immobilization of TiO$_2$ on RHS adsorbent, contact time, nanoparticle mass and initial concentration of dye in removal efficiency were investigated. The results of this research showed that with an increase in pH and alkalinity of the solution, the removal efficiency declined. As the pH changed from 3 to 9, the removal efficiency in UV/TiO$_2$/RHS, RHS adsorbent and UV$_C$ radiation declined from 75.25 to 27.87, 8.37 to 3.4, and 16.62 to 3.25%, respectively. The maximum dye removal efficiency obtained by UV/TiO$_2$/RHS was as large as 87.5% under pH=3, contact time of 60 min, nanoparticle mass of 1 g/L, and 25 mg/L concentration of the reactive red 198 dye. Therefore, the rice husk silica as a natural adsorbent in combination with (TiO$_2$/UV) can be used as an effective method for removal reactive red of aqueous solutions on a larger scale by optimizing the parameters affecting the removal efficiency.

*Keywords*: Photocatalyst, Rice husk silica, Reactive red 198, Removal efficiency.

## 1. Introduction

Dye pollutants from the textile industry are important sources of environmental contamination. It is estimated that from 1 to 15% of the dye is lost during dyeing processes and is released in wastewaters [1]. In the textile dyeing process, only 85% of the coloring matter gets fixed to cloths, while the remaining 15% of dyes are discarded from dye baths as effluent [2]. Dyes are divided into different types including azo, phythane, acridine, xanthine, flavin, anthraquinones, and cyanine according to chemical structure. Alternatively, they can be divided into reactive, bending, straight, acidic, and dispersed types in terms of application [3]. Some of the dyes and pesticides contain a poisonous quality which has an impact on a variety of organs in human beings [4]. In inorganic chemistry, azo dye compounds are a class of dyes with certain properties which are now being considered for various aspects such as colorants for digital printing and photography, liquid crystals,

chiral receptors, dyes for drug, food and cosmetic applications and organic synthesis [5]. Reactive dyes are a group of azo dyes widely used in textile industry [6]. Reactive dyes are important commercial synthetic dyes and used in the basic fabric exports in the textile industry. Also, their colors are retained under exposure to the sunlight and high solubility in water [7]. Dyes are not only unbiodegradable but also toxic, carcinogenic and mutagenic [8-11]. The presence of dyes causes contamination of aqueous resources. Furthermore, they prevent permeation of sunlight and decrease oxygen, thereby causing serious damage to the environment through the death of the living creatures [12, 13]. During the degradation process of some dyes, e.g. azo dyes, aromatic amines are produced which are potentially carcinogenic and mutagenic [14]. Therefore, it is necessary that the wastewaters containing dyes be treated before discharging into the environment through the suitable options. Some of the methods for treatment including coagulation are not effective enough due to incomplete degradation of the compounds, and they transfer dye compounds from one phase to another [15].

*Corresponding author.
E-mail address: hrnassehi@semums.ac.ir (H. Nassehinia)

AOPs are a group of processes that are predicated on the generation of hydroxyl radicals. These radicals are highly reactive, leading to the total mineralization of most of the organic pollutants. Nanocrystalline materials mediated semiconducting photocatalysis are expeditiously becoming an efficient AOP, in which semiconductor material absorbs greater energy than its band gap energy which leads to the excitation of electrons from the valence band to the conduction band, consequently engendering electrons and holes. The valence band holes react with the water molecules and hydroxide ions to form hydroxyl radicals whereas the electron reacts with oxygen molecules and form superoxide radicals. These free radicals are extremely proficient oxidizers of organic dyes which can attack organic dyes and degrade them into $CO_2$ and $H_2O$ [4].

Recently, considerable attention has been focused on the use of semiconductors as a mean to oxidize toxic organic chemicals. Photocatalysis is a promising technique for the degradation of inorganic and organic pollutants in air and water. Especially, semiconductor oxides such as ZnO, CuO, $MnO-Ag_2O$ and $TiO_2$ have been recognized to be preferred materials for photocatalytic processes, due to their high photosensitivity, non-toxic nature, low cost and chemical stability [16-18]. The reasons for the extensive use of $TiO_2$ for photocatalytic removal of contaminants in aqueous solutions include ultraviolet adsorption and the highest stability among advanced oxidation processes [19]. Immobilizing of $TiO_2$ on the support materials results in better filtration and less material loss, resulting in increased photocatalytic degradation rates [20]. Immobilization of various nanoscopic substances from ion/molecule, a polymer to a particle in porous solids has been a topic of interest of materials chemistry and the application of the resulting hybrids in such areas as a catalyst, drug carrier, adsorbent, etc. has been examined. Due to the useful functions of titanium dioxide ($TiO_2$) as white pigment, UV absorber, catalyst/photocatalyst and so on, the preparation and characterization of $TiO_2$ with varied phases (anatase, rutile, etc.), macroscopic morphology (film, powders) and nanoscopic organization (shape/size of the domain/particles) have been reported extensively [21]. The environmentally friendly nature of $TiO_2$ (natural abundance, non-toxic and chemically stable) makes it more attractive for a wide range of practical applications. As to the $TiO_2$ nanoparticle, the particle aggregation is a drawback for an application. For the catalyst application of $TiO_2$ nanoparticle, the collection from the suspension after the catalytic reactions is another issue

to be solved. As a way of functional materials' design of $TiO_2$ nanoparticle, the immobilization of $TiO_2$ in various nano spaces has been reported so far. Supported $TiO_2$ nanoparticle may behave differently from un-supported ones for aggregation and dispersion [21]. The supported $TiO_2$ on the various materials such as zeolite, activated carbon and etc. has been studied in the photodegradation of organic pollutants such as dyes [22]. The results of various researches suggest that in the adsorbents mixed with nanoparticles, not only the number of optical active sites increases, but also it causes increasing photocatalytic characteristics due to the closeness of adsorption sites to optical active sites [23]. Among support materials, immobilization of $TiO_2$ on silica materials has been commonly proposed [24]. One of the byproducts of the rice production process is rice husk whose silica content is considerable [25]. Silica is known as one of the most important adsorbents which adsorbs contaminants [19]. Preparation and production of adsorbent out of rice husk is far less expensive, and its cost is around 1% of the cost of producing commercial activated carbon [26]. Since nano photocatalyst of ultraviolet and titanium dioxide compounds and rice husk silica adsorbent have not been yet used to remove the color, this study was performed with the aim of investigating the efficiency of the UV/TiO2/RHS in removing reactive red 198 dye from a synthetic aqueous solution and determining the optimal conditions while investigating the parameters influencing the removal of dye. Furthermore, in order to determine the effect of immobilization of $TiO_2$ on RHS, the efficiency of the mentioned compound was compared to RHS adsorbent and $UV_C$ radiation alone at similar conditions.

## 2. Experimental

### 2.1. Chemicals

The reactive red 198 dye used in this research was prepared from Alvan Sabet Co. with the following specifications: (molecular weight: 968.21 gr/mole and chemical formula: $C_{27}H_{18}ClN_7Na_4O_{15}S_5$) [27]. The $TiO_2$ catalyst with the mean particle size of around 21 nm and a purity of 99.5% with a pacific area of 50 $g/m^2$ was supplied from Degussa Co [28]. Fig. 1 demonstrates the chemical structure of the reactive red 198 dye. The other chemicals used in this study, including sodium hydroxide (NaOH), sulfuric acid ($H_2SO_4$), nitric acid ($HNO_3$) and ethanol ($C_2H_6O$) were supplied from Merck Co.
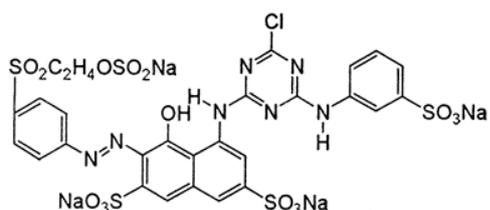
**Fig. 1.** The chemical structure of the reactive red 198 dye.

## 2.2. Preparing silica from rice husk

In order to prepare RHS, the raw husk was prepared from the rice field factories in the north of Iran, and rice husk was then exposed to 110 °C in an oven for 24 h after washing it. Then, following the acid washing stage (acid washing by HCl 3% and sulfuric acid 10% with a ratio of 50 g of husk with one liter of the mixture of these two acids for 2 h), it was washed by distilled water. Next, it was dried in an oven at 100 °C for 4 h. Silica was eventually prepared in a furnace (Model: SEF-202P, Korea) with a temperature of 800 °C for 4 h [25].

## 2.3. Immobilization of titanium dioxide on RHS

The titanium dioxide solution was prepared by adding 1.5 g of $TiO_2$ made by Degussa Co. in 180 ml of ethanol, where the titanium dioxide powder was first dispersed completely in ethanol and a cloudy state was developed in the solution.

Next, 1.5 ml of diluted nitric acid with pH=3.5 was added for dispersing $TiO_2$. Following the addition of the acid, the cloudy texture of the solution was disappeared. Thereafter, a slurry was placed inside the ultrasonic device (Model: UW 2070, Germany) with a frequency of 59 kHz for 5 min for separating the $TiO_2$ lumps and obtaining a clear solution, so that it would be suitable for the deposition process. Then, by adding the titanium dioxide solution to RHS adsorbent and depositing by a deep coating method, the compound was dried at room temperature for 1 d. Finally, the coated silica was prepared after being placed in a furnace at 450 °C for 1 h [29].

## 2.4. Characterization

In order to investigate the morphology of the sample surface (RHS before and after the immobilization of the nanoparticles) and understand immobilization of nanoparticles on the RHS adsorbent, a Scanning Electron Microscope (SEM) analysis was performed in Sharif University of Technology in Tehran. The crystal structure of the $TiO_2$ nanoparticles was also determined using an X-ray diffraction (XRD) device at Damghan University.

## 2.5. Dye removal procedure

In this study, removal of reactive red 198 dye was done in batch reactors with a volume of 250 ml using titanium dioxide deposited RHS in the presence of a lamp with power of 9 watt and size of 13 cm of $UV_C$ type with a wavelength of 220-230 nm of Philips Co. as the radiation source. This lamp with a closed-end quartz coating with a diameter of 25 mm was placed inside the solution on the magnetic stirrer. Any thermal effect caused by the lamps was controlled by a larger reactor with a volume of 1 L with water content in the external part. In order to prevent the radiation of the beam of $UV_C$ lamp from exiting the reactor and for effective radiation, the entire surrounding of the reactor was covered by aluminum foil. The general schema of the reactor is shown in Fig. 2. The stock solution of the dye with a concentration of 100 mg/L was prepared by dissolving 0.1 g of the reactive red 198 dye in deionized water, with the solution being kept in darkness. In order to examine the efficiency of the $UV/TiO_2/RHS$ and determine the effect of immobilization of titanium dioxide on RHS, the removal efficiency was compared across three different methods:

a) The $UV/TiO_2/RHS$, b) the RHS adsorbent and c) $UV_C$ radiation alone. In (a) and (b) methods, different conditions [pHs (3-5-7-9), different contact times (30-60-90 min), different nano photo catalyst mass (0.5-1-1.5 g), and different concentrations of the reactive red 198 dye (25-50-75-100 mg/L)] and in (c) method, under similar conditions but without the mass of the materials, were investigated.

Before turning on the $UV_C$ lamp, adsorption of the dye by the deposited silica adsorbent was investigated in darkness [30]. During the experiment, the solution was stirred constantly by a magnetic stirrer (with a rate of 150 rpm).

The effect of pH was studied at a concentration of 50 mg/L of the dye solution, nano photo catalyst mass of 1 g/L and contact time of 60 min, where the optimal pH was determined. Using sulfuric acid and NaOH 1 N, the solution pH was adjusted. Investigating the effect of time on the removal efficiency was done under optimal pH conditions obtained from the previous stage, a solution concentration of 50 mg/L and a nano photo catalyst mass of 1 g/L.

To determine the optimal dose, solutions with a concentration of 50 g/L, an optimal pH and a contact time of 60 min were also used. Eventually, by considering the optimal pH, the contact time of 60 min and the nano photo catalyst mass of 1 g/L, the effect of the concentration of the dye on removal efficiency was examined. Before analysis, the samples were filtered by
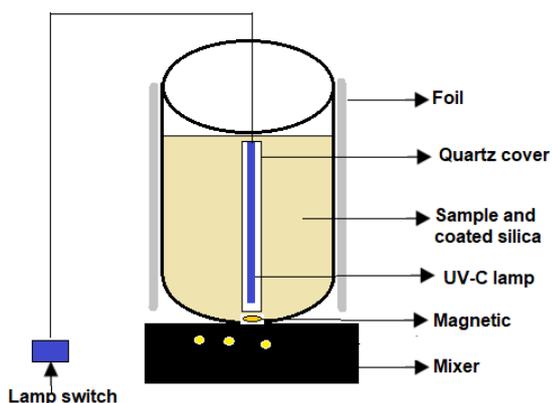
**Fig. 2.** The general schematic of fabrication of the reactor pilot in this study.

a centrifuge device to remove turbidity. Next, using the spectrophotometer (Model: SP-300) at a wavelength of 518 nm, the concentration of the samples was determined [2]. All of the experiments were conducted under the same experimental conditions at $25 \pm 2$ °C.

## 3. Results and Discussion

### 3.1. Characterization

#### 3.1.1. Structural analysis of the catalysts

The SEM pattern of RHS before and after the immobilization of the nanoparticles has been shown in Fig. 3. The immobilization of nanoparticles (Fig. 3b-2) and lack of change in the morphology of husk silica (Fig. 3b-1) show the results of operation of $TiO_2$ deposition. The $TiO_2$ particles were dispersed fairly uniform on rice husk silica because the $TiO_2$ nanoparticles were dispersed homogeneously in the solution before coating. The results indicated that the surface properties of RHS before and after the immobilization of the nanoparticles had no significant difference due to the presence of $TiO_2$ nanoparticles. Furthermore, a major portion of $TiO_2$ particles have been loaded onto the surface and have not been rejected in the pores, thereby the possibility of permeation of

light onto the $TiO_2$ surface increased. The SEM images show that $TiO_2$ nanoparticles are mesoporous and crystalline, and have a rough surface area. A rough surface is more photocatalytically active compared to smooth surfaces. A rough surface displays a higher surface area, leading to more photocatalytic sites, thus these microspores were sufficient to influence the photocatalytic activity of $TiO_2$ nanoparticles.

#### 3.1.2. XRD analysis

The crystal structure of $TiO_2$ nanoparticles was determined by XRD device and the results are demonstrated in Fig. 4. In the XRD pattern, anatase and rutile phases existed in the crystal structure of $TiO_2$.

The observed diffraction pattern of $TiO_2$ in $2\theta$ (25.3), (37.8), (48.1), (53.9) and (55.1) belongs to anatase. All peaks can be well indexed to wurtzite type crystal structure (tetragonal phase) with lattice constants of a=0.37830 nm and c=0.95100 nm. The crystallite sizes were calculated using Debye- Scherrer's equation: $D = 0.9 \lambda / (\beta \cos\theta)$ where D is crystallite size, $\lambda$ is the X-ray wavelength (1.54A°), $\beta$ is the full-width at the half maximum intensity of the diffraction line and $\theta$ is the diffraction angle [4, 32]. The crystallites sizes were estimated to be around 20 nm.

### 3.2. Photodegradation

The five important factors which mostly affect the degradation efficiency were: the effect of pH, the immobilization of $TiO_2$ on RHS, the contact time, the mass of photocatalyst and the concentration of dye.

#### 3.2.1. The effect of pH

The pH solution plays a major role in the efficiency of removal processes including photocatalytic and adsorption processes through influencing the chemical structure of the dye, the superficial charge of the adsorbent, the chemistry of the solution, the separation of functional groups at active sites of the adsorbent [3], and superficial charge of the nanoparticles [31].
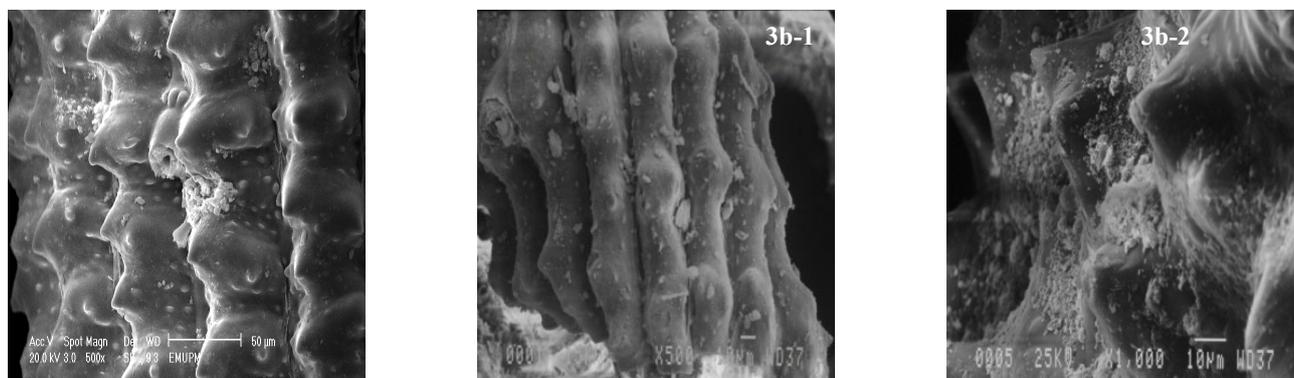


**Fig. 3.** a) SEM pattern of RHS before the immobilization b) SEM pattern of RHS after the immobilization.
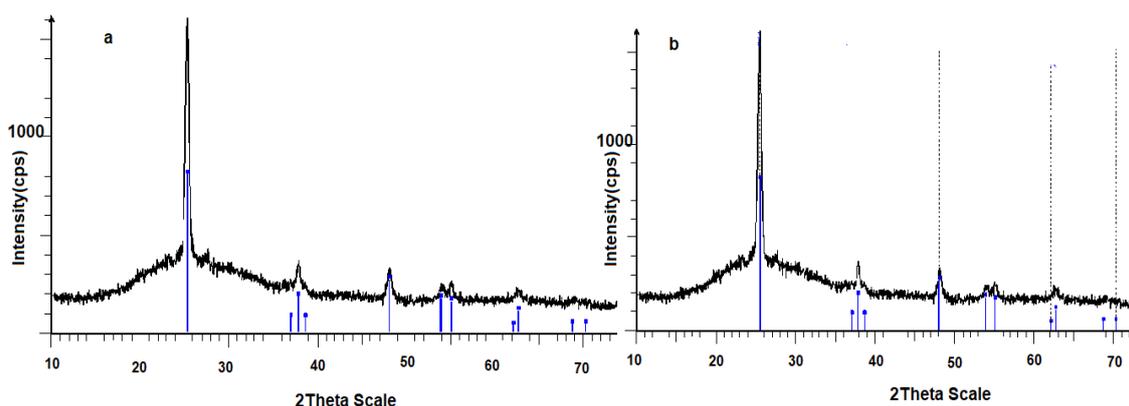
**Fig. 4.** The XRD pattern of $TiO_2$ nanoparticles a) before the immobilization, b) after the immobilization.

To determine the effect of pH, specify the optimal pH, and understand the effect of immobilization of $TiO_2$ on RHS in the removal efficiency in this study, a stock solution of 100 mg/L of reactive red 198 dye solution with a concentration of 50 mg/L was prepared and the removal efficiency was investigated across three different methods (UV/$TiO_2$/RHS, RHS adsorbent, and $UV_C$ radiation alone). The pH of the aqueous solution was examined within the range of 3-9. The results of this research showed that with increasing the pH and alkalinity of the solution, the removal efficiency declines, such that as the pH changes from 3 to 9, the removal efficiency in UV/$TiO_2$/RHS, RHS adsorbent and $UV_C$ radiation alone declines from 75.25 to 27.87, 8.37 to 3.4, and 16.62 to 3.25%, respectively. This means that in all of the three states, with increasing the pH, the removal efficiency diminishes. The optimal pH for continuing the experiments was determined to be 3. Furthermore, the UV/$TiO_2$/RHS indicated the greatest efficiency, while the RHS adsorbent showed the lowest efficiency (Fig. 5).
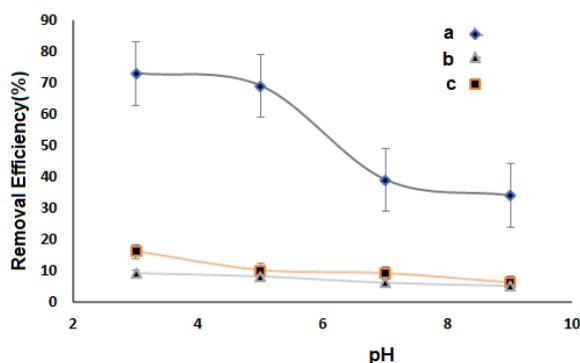


**Fig. 5.** The removal efficiency of the reactive red 198 dye under the following conditions a) UV/$TiO_2$/RHS at contact time of 60 min, materials dose of 1 g/L and concentration of 50 mg/L b) RHS adsorbent at contact time of 60 min, materials dose of 1 g/L and concentration of 50 mg/L c) UV-C radiation alone at contact time of 60 min and concentration of 50 mg/L.

Degradation of the reactive red 198 dye by the studied methods is heavily influenced by the solution pH, such that the maximum removal of the dye took place at pH=3 for all of the three methods. Similar results in several studies, have been reported by researchers [33].

It seems that as the pH increases, due to ionization of functional groups such as hydroxyl, negative charge is developed across the surface of nanoparticles (Eq. 1), whereby an electrostatic repulsion is developed between the surface of the nanoparticles with a negative charge and the molecules of reactive red 198 dye with a negative charge. However, with reducing the solution pH, the number of sites with positive charge on the surface of nanoparticles (Eq. 2) and the adsorbent's surface [33] increases and an electrostatic attraction develops between the site with positive charge on the surface of nanoparticles and the adsorbent and the molecules of reactive red 198 dye with a negative charge. In turn, with further adsorption of dye molecules, photocatalytic removal increases [34].

$$TiOH + OH^- \rightarrow TiO^- + H_2O \qquad (1)$$

$$TiOH + H^+ \rightarrow TiOH_2^+ \qquad (2)$$

Bazrafshan *et al.* have reported the maximum removal of reactive red 198 dye at pH=2 using the ash obtained from pistachio wastes. They have also reported the decreased removal of reactive red 198 dye with an increase in pH from 4 to 10 using $TiO_2$/$UV_C$ [35]. The pH changes cause a change in the photocatalytic surface charge and adsorption of the reactive red 198 dye molecule on the catalyst surface. The PZC of $TiO_2$ is around 6.8. At a pH level of less than 6.8, the catalyst surface is positively charged. Also, at lower pH, more hydroxyl radicals are produced, leading to an increase in the photocatalytic degradation rate. An increase in pH increases the number of sites with a negative charge. Therefore, the negative sites on the catalyst surface are not effective enough to absorb the red dye anions [7].

At a pH level of less than 6.8, where pH < PZC $TiO_2$, the surface of $TiO_2$ mainly present in the forms of Ti-OH and/or $Ti-OH_2^+$, resulting in the formation of hydrogen bonds with the reactive red 198 dye molecules. In addition, the reactive red 198 dye is a polar molecule, and it could be adsorbed on the surface of $TiO_2$ via van der Waals force. On the other hand, O, N and S atoms in the reactive red 198 dye could form hydrogen bonds due to their high electronegativity with the surface hydroxyl groups of $TiO_2$. Therefore, at a pH level of less than 6.8, we think that both the van der waals force and the hydrogen bond formation are contributive to the reactive red 198 dye adsorption. At a pH level of upper than 6.8, where pH > PZC, the surface hydroxyl groups of $TiO_2$ will be dissociated to form $TiO^\circ$; thus, electrostatic repulsion between negatively charged dye molecules and $TiO^\circ$ is obtained, leading to the lower adsorption capacity. Then the adsorbed percentage for dye in the low pH region is greater than that of high pH region [36, 37].

### 3.2.2. The effect of immobilization of TiO₂ on RHS

$TiO_2$ has been immobilized in/on various porous hosts including clays and clay minerals, silica gels, porous inorganic membranes, zeolites, and even in some metal-organic frameworks. Porous hosts are expected to play a role in controlling the shape and size of $TiO_2$ nanoparticle. Among porous hosts used so far, porous silica has several advantageous aspects such as the shape and the size of the pore in the size range of up to 10 nm and the reactivity of the pore not only as the template for the syntheses of $TiO_2$ nanoparticle but also for the application of the products after the hybridization with $TiO_2$ nanoparticle. Furthermore, the uses of organic modified porous silica, which have been used for controlled adsorption and the visible light absorption, for the immobilization of $TiO_2$ are also worth investigating to obtain multi-functional hybrid materials as well as to optimize the function as catalysts [21]. Based on the data obtained from the results of investigations across the three mentioned methods, the degree of removal of reactive red 198 dye by UV/$TiO_2$/RHS is greater than RHS adsorbent and $UV_C$ radiation alone methods. It can be attributed to titanium dioxide nanoparticles on the surface of RHS, which is in line with the results of the study by Janie and the colleague [15]. Furthermore, considering the results of the data regarding the catalytic $UV_C$ radiation method in comparison with the method without $UV_C$, it is understood that photocatalytic methods have a great contribution in removing dyes from aqueous compared to adsorption.

The greater efficiency of UV/$TiO_2$/RHS might be attributed to reasons including enumeration of the number of optical active sites as $TiO_2$ nanoparticles settle on the surface of silica, of contaminants on the surface of silica due to absorptivity of silica and closeness of adsorption sites to optical active sites. Furthermore, in the $TiO_2$ immobilized method, not only the light dispersion by the particles is less, but the depth of permeation of light is also less due to a thinner layer of the fluid on the surface of nanoparticles [15].The degradation mechanism of the dye involves activation of $TiO_2$ nanoparticles with radiation of rays, whereby its electrons are stimulated from the capacity band to the conduction band, after which hydroxyl radicals are produced. These radicals are strong oxidative agents and attack to the organic contaminants adjacent to the surface of $TiO_2$, thereby causing degradation of the dye's molecules.

Significant Reactive dye degradation rate by UV/$TiO_2$/RHS is obtained from the photocatalysis mechanism, and it is adversely correlated with the specific surface area data. The reaction is done by adsorption of a photon with enough energy. The adsorption leads to a charge transfer, resulting from the transfer of electrons from the valence band to the conduction band of the semiconductor, so that the holes are generated in the valence band. Between the generated holes, the hole with one reductant is generated by the oxidant products. The generated electrons react with water molecules and convert them into hydroxyl radicals [4]. This means that the presence of $TiO_2$ conducts the Photocatalysis and furthermore this assumption is also strengthened by its comparison with photooxidation and photodegradation.

The higher degradation rate of dye over photooxidation compared to photodegradation is caused by the presence of $H_2O_2$ as an oxidant in the photocatalytic system by the following mechanism:

$$O_2 + e^- \rightarrow O_2^{\bullet-} \tag{3}$$

$$O_2^{\bullet-} + H^+ \rightarrow HO_2^{\bullet} \tag{4}$$

$$HO_2^{\bullet} + HO_2^{\bullet} \rightarrow H_2O_2 + O_2 \tag{5}$$

$$O_2^{\bullet-} + HO_2^{\bullet} + H^+ \rightarrow H_2O_2 + O_2 \tag{6}$$
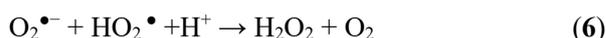
As the radicals formed from the interaction between $TiO_2$ and UV light under the solvent environment, its formation was accelerated by the presence of $H_2O_2$ which the propagation reaction can occur easily [38].

In this course of degradation, first double bonds of N=N present in dyes are broken and then are converted to intermediate compounds and eventually change into mineral compounds including $N_2$, $CO_2$, and $H_2O$.

Fig. 6. shows the different stages of the proceeding of photocatalytic reaction across the surface of nanoparticles [39].

In many studies, researchers have reported a significant increase in the removal efficiency by immobilizing catalyst on a support adsorbent in comparison with support adsorbent and slurry $TiO_2$ [40]. In a study done by Rismanchian *et al.* on investigation of the photocatalytic activity in $TiO_2$/Zeolite and $TiO_2$ states in removing safranin dye, they have reported that the photocatalytic activity of $TiO_2$ coated by zeolite is greater than that of the photocatalyst alone, whereas with the initial concentration of 50 mg/L of the dye, the removal efficiency by $TiO_2$/zeolite and $TiO_2$ has been 69.63 and 10.49%, respectively [23].

### 3.2.3. The effect of contact time

The removal efficiency of the studied dye for UV/$TiO_2$/RHS and $UV_C$ radiation alone grew with prolongation of the time (Fig. 7). The degree of removal in the combined method was been greater in the early minutes, while over time it took place with a less dramatic trend, such that the removal efficiency for the mentioned method increased from 48.87 to 75.25% in the first 60 min, from 48.87 to 80.5% within 90 min, when compared to the contact time of 30 min. However, for the $UV_C$ alone method, the removal of dye (30.5%) within 90 min in comparison with 30 min (5.62%) showed. The removal efficiency in the RHS adsorbent method increased with prolongation of time up to the first 75 min, such that the removal efficiency increased from 6.87 to 9.5%. Thereafter, prolongation of the contact time had no effect on degradation efficiency, where it showed a degradation efficiency of 8.37% within the contact time of 90 min. The degree of dye removal in this study in the combined and $UV_C$ radiation alone methods increased with the prolongation of contact time.
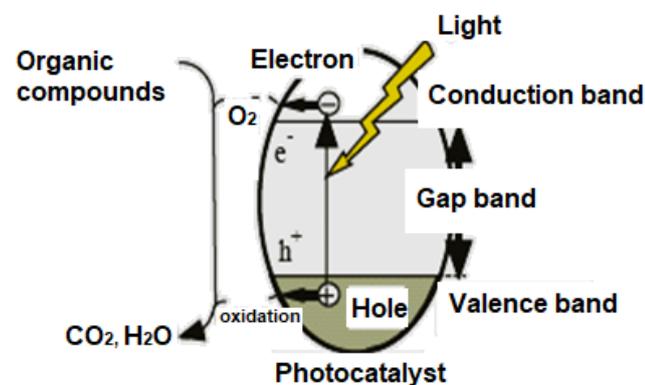
The reason can be attributed to further production of the active radicals of hydroxyl and sufficient time for the reaction and degradation of the dye molecules by the hydroxyl active radicals over time. On the other hand, the degree of dye removal in the combined method grew less dramatically when compared with the early minutes, possibly due to the reduction in the concentration of the solution's dye and a number of active sites over time. In the study by Rismanchian *et al.* with prolongation of time, the degree of dye removal was also greater and the extent of dye removal at longer times grew less dramatically when compared with early minutes [23]. The degradation efficiency in the RHS adsorbent method has increased with prolongation of time up to the first 75 min, after which prolongation of time has no effect on the elevation of the degradation efficiency.

### 3.2.4. The effect of the nano photocatalyst mass

One of the most important issues that should be taken into consideration in studying removal using adsorbents and photocatalysts is determining the suitable mass, which was another parameter that was investigated. Fig. 8 indicates the effect of the initial mass of the nano photocatalyst on degradation efficiency of reactive red 198 dye under pH=3, contact time of 60 min with dye's initial concentration of 50 mg/L. As it indicates, the photo decolorization rate of reactive red 198 dye increases with increasing the initial mass of the catalyst, such that it increased to 66.5% at the initial mass of 0.5 g/L of the nano photocatalyst, at 1.5 g/L, it increased to 82.12% in UV/$TiO_2$/RHS, and in RHS adsorbent method it increased from 6.12 to 9.25%.
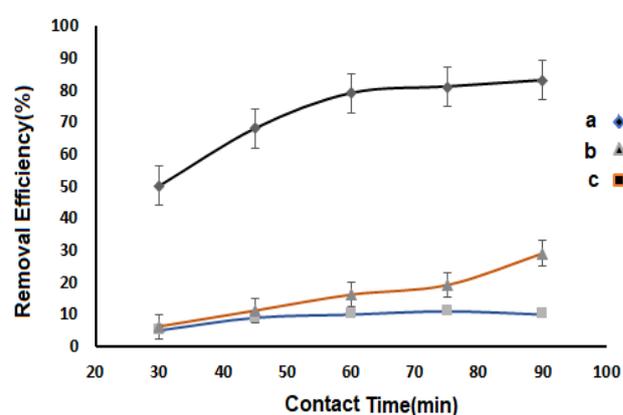


**Fig. 7.** The degradation efficiency of the reactive red 198 dye under the following conditions a) UV/$TiO_2$/RHS at pH=3, materials dose of 1 g/L and concentration of 50 mg/L. b) RHS adsorbent at pH= 3, materials dose of 1 g/L and concentration of 50. c) UV-C radiation alone at pH=3 and concentration of 50 mg/L.



**Fig. 6.** The different stages of the proceeding of photocatalytic reaction across the surface of nanoparticles.

It is due to the fact that in primary stages a large number of empty surface sites of the adsorbent are available for adsorption, but over time the empty superficial sites remained in adsorption of dye face a problem due to the repulsive force developed between the dye molecules of the solid surface and the soluble phase [35]. The increased contact area between the deposited adsorbent and the contaminant, enumeration of active sites, and production of free electrons in the conductive band are the reasons of elevation of removal efficiency with increasing the nano photocatalyst mass. The photodecomposition rate of the organic pollutant is influenced by the number of active sites as well as the light absorption ability of the photocatalyst. For a suitable high concentration of the catalyst, the degradation occurs rapidly because of generating more $h_{vb}^+$ and $e_{cb}^-$ [38, 41]. In this regard, an increase in the degradation efficiency with a growth in the nano photocatalyst mass has been reported. Development of the efficiency is usually considered as a positive effect, but the development of turbidity and in turn the diminished intensity of UV light and the reduced production of hydroxyl radical should be considered as a negative effect at a high initial mass of the nano photocatalyst so that the negative effect does not outweigh the positive effect [34].

### 3.2.5. The effect of concentration

Another parameter that contributes to the degradation efficiency of adsorption and photocatalytic processes is the initial concentration. In this study, the effect of the initial concentration of the dye (25-50-75-100 mg/L) on the removal efficiency for UV/TiO$_2$/RHS, RHS adsorbent and UV-C radiation alone was investigated by keeping other parameters constant.
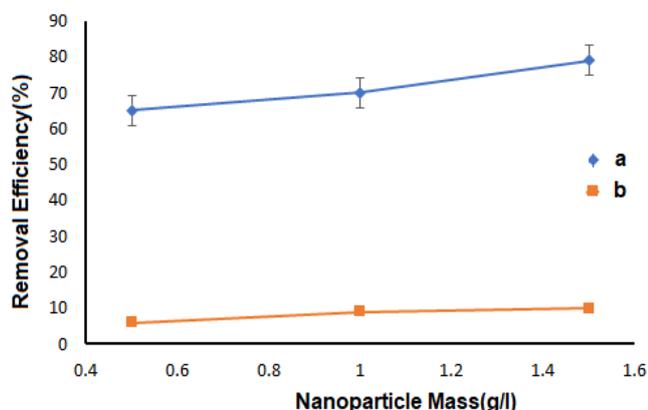
Considering the data obtained from investigation of the effect of concentration on removal efficiency, with increasing the initial concentration, i.e. from 25 to 100 mg/L, in all of the three methods the efficiency diminished, such that the initial concentration had a great contribution` in removal efficiency. By changing the initial concentration of the solution from 25 to 100 mg/L, the dye's removal efficiency in UV/TiO$_2$/RHS, RHS adsorbent, and UV-C radiation alone methods decreased from 87.5 to 38.19, 12.25 to 3.18, and 21 to 2.75%, respectively. The greatest removal by UV/TiO$_2$/RHS was obtained to be 87.5% at 25 mg/L (Fig. 9). The results obtained from investigating the effect of the initial concentration on removal efficiency indicated that with increasing the initial concentration of the solution dye, the removal efficiency diminishes, which is in line with the studies done on degradation efficiency by adsorption and photocatalytic methods [38]. Because of the increased dye concentration in the solutions, the accessible catalyst surface to the light is restricted. At high concentrations, the occupied positions on the catalyst surface by the dye molecules can limit the available active sites for photons. In addition, more photons can be absorbed by copious reactive red 198 molecules, leading to fewer photons for excitation of semiconductors present on the catalyst surface. Finally, lesser hydroxyl radicals can be produced at high reactive red 198 concentration leading to a decrease in decolorization efficiency [7].

The reason of the reduction in the efficiency can be the fact that at a constant dose, with an increase in the initial concentration of the dye, the extent of the available active area remains constant, but the number of contaminant's moles present in the reaction environment has grown.



**Fig. 8.** The degradation efficiency of the reactive red 198 dye under the following conditions. a) UV/TiO$_2$/RHS at pH=3, contact time of 60 min and concentration of 50 mg/L. b) RHS adsorbent at pH= 3, contact time of 60 min and concentration of 50 mg/L.
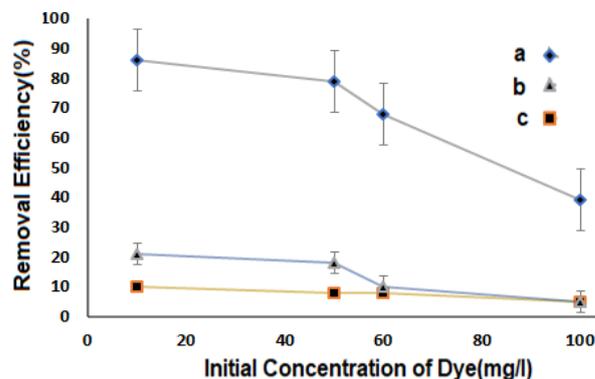


**Fig. 9.** The degradation efficiency of the reactive red 198 dye under the following conditions a) UV/TiO$_2$/RHS at pH= 3, contact time of 60 min, and materials dose of 1 g/L b) RHS adsorbent at pH=3, contact time of 60 min, and materials dose of 1 g/L. c) UV-C radiation alone at pH=3 and contact time of 60 min.

In other words, the deposited adsorbent has a limited number of active sites which become saturated at higher concentrations. In addition, it is due to the elevation of the concentration of the intermediate compounds resulting from degradation of the dyes and their competition for the main dyes for absorbing photons. Furthermore, higher concentrations of the contaminant and the intermediates resulting from degradation of the contaminant cause a reduction in the number of hydroxyl radicals for oxidation and diminish access of the active sites of the catalyst to light. Indeed, the presence of dye molecules causes light dispersion which in turn brings about the diminished activity of the catalyst and lowered removal of the dye [37].

## 4. Conclusions

In this study, the efficiency of $UV/TiO_2/RHS$ in removing reactive red 198 dye was investigated following deposition and immobilization of $TiO_2$ on Rice Husk Silica under different conditions, followed by an examination of the effect of $TiO_2$ deposition on the adsorbent. In this research $UV/TiO_2/RHS$ had higher degradation efficiency in comparison with RHS adsorbent and $UV_C$ radiation alone. Therefore, rice husk silica can be used as a suitable support for $TiO_2$ and removal of dye. The best conditions for dye removal of the $UV/TiO_2/RHS$ were obtained at pH=3, contact time of 60 min, and initial concentration of the dye as low as 25 mg/L. Furthermore, the solution pH showed a greater impact on removal efficiency compared to other parameters. The maximum dye removal efficiency was obtained by $UV/TiO_2/RHS$ and was as much as 87.5% under pH=3, contact time of 60 min, nanophotocatalyst mass of 1 g/L, and a concentration of 25 mg/L of the reactive red 198 dye. The removal efficiency of the studied dye for $UV/TiO_2/RHS$ and $UV_C$ radiation alone grew with the prolongation of the time. The findings of the study suggest that by optimizing the parameters influencing the removal efficiency, RHS can also be used as a natural adsorbent in combination with $(TiO_2/UV)$ as an environmentally friendly method for removing reactive red 198 dye from aqueous solutions at larger scales.

## Acknowledgements

## References

[1] L. Shabani, H. Aliyan, Iran. J. Catal. 6 (2016) 221-228.

[2] P. Aravind, H. Selvaraj, S. Ferro, M. Sundaram, J. Hazard. Mater. 318 (2016) 203–215.

[3] A. Buthiyappan, A.R. Abdul Aziz, W.M. Ashri, W. Daud, Rev. Chem. Eng. 32 (2016) 1-47.

[4] S.D. Khairnar, M.R. Patil, V.S. Shrivastava, Iran. J. Catal. 8 (2018) 143-150.

[5] A. Bamoniri, B.F. Mirjalili, N.Y. Mahabadi, Iran. J. Catal. 8 (2018) 81-88.

[6] M. Ahmadi, K. Rahmani, A. Rahmani, H. Rahmani, Pol. J. Chem. Technol. 19 (2017) 104-112.

[7] N.E. Fard, R. Fazaeli, Iran. J. Catal. 8 (2018) 133-141.

[8] M. Farzadkia, K. Rahmani, M. Gholami, A. Esrafili, A. Rahmani, H. Rahmani, Korean J Chem. Eng. 31 (2014) 2014-2019.

[9] M. Fazlzadeh, A. Rahmani, H. Nassehinia, H. Rahmani, K. Rahmani, Koomesh 3(2016) 350-356.

[10] M. Gholami, K. Rahmani, A. Rahmani, H. Rahmani, A. Esrafili, Desalin. Water Treat. 57 (2016) 13878-13886.

[11] P. Mahajan, J. Kaushal, Coord. Chem. Rev. 1 (2014) 67-76.

[12] S. Dianat, Iran. J. Catal. 8 (2018) 121-132.

[13] A. Yazdanbakhsh, A. Rahmani, M. Massoudinejad, M. Jafari, M. Dashtdar, Desalin. Water Treat. 57 (2016) 23719-23727.

[14] A. Maleki, Y. Zandsalimi, M. Jafari, H. Daraei, S. Sadeghi, J. Health. 6 (2016) 498-506.

[15] S. Alijani, M. Vaez, A. Zaringhalam Moghadam, Int. J. Hydrogen Energy 6 (2013)243-256.

[16] H. Nassehinia, A. Rahmani, G. Ghaieny, S.M. Mehdinia, Koomesh 18 (2016) 309-316.

[17] J. Esmaili-Hafshejani, A. Nezamzadeh-Ejhieh, J. Hazard. Mater. 316 (2016) 194–203.

[18] M. Karimi-Shamsabadi, A. Nezamzadeh-Ejhieh, J. Mol. Catal. A: Chem. 418–419 (2016) 103–114.

[19] L. Pereira, R. Pereira, C.S. Oliveira, L. Apostol, M.Gavrilescu, M.N. Pons, O. Zahraa, J. Photochem. Photobiol. 89 (2013) 33-39.

[20] O.K. Mahadwad, P.A. Parikh, R.V. Jasra, C. Patil, Environ. Technol. 33 (2012) 307-312.

[21] K.G. Vibulyaseak, S.B. Deepracha, M. Ogawa, J. Solid State Chem. 270 (2019) 162-172.

[22] X. Xiu-qin, J. Rong-li, S. Hong-kai, Q. Ke-di, W. Peng, W. Jing, J. Adv. Oxid. Technol. 19 (2016) 381-386.

[23] M. Rismanchian, S. Barakat, N. Khoshzat, R. Keshavarzi, M. Shakerian, Int. J. Env. Health Eng. 4 (2015) 1-7.

[24] H. Nassehinia, A. Mahmoodi, S.M. Mehdinia, Koomesh 18 (2016) 334-342.

[25] S.M. Mehdinia, P. Abdul Latif, A. Makmom Abdullah, H. Taghipour, Asian J. Sci. Res. 4 (2011) 246-254.

[26] S.M. Mehdinia, K. Moeinian, Rastgoo, Iranica J. Energy Environ. 5 (2014) 218-223.

[27] M.A. Zazouli, D. Balarak, Y. Mahdavi, M. Ebrahimi, Iran. J. Health Sci. 1 (2010) 36-43.

[28] M. Gholami, H. Nassehinia, A. Jonidi-Jafari, S. Nasseri, A. Esrafili, J. Environ. Health. Sci. Eng. 12 (2014) Article 45.

[29] S.N. Hosseini, S.M. Borghei, M. Vossoughi, N. Taghavinia, Appl. Catal. B. 74 (2007) 53-62.

[30] J. Matos, M. Hofman, R. Pietrzak, Carbon 54 (2013) 460-471.

[31] C.R. Marcelo, G.A. Puiatti, M.A. Nascimento, A.F. Oliveria, R.P. Lopes, J. Nanomater. (2018) Article ID 4642038.

[32] A. Nezamzadeh-Ejhieh, S. Tavakoli-Ghinani, C.R. Chim. 17 (2014) 49-61.

[33] M. Dehghani, M. Ghadami, T. Gholami, M.A. Shiri, Z. Elhameyan, M.R. Javaheri, N. Shamsedini, S. Shahsavani, J. Health Sci. Surveillance Syst. 3 (2013) 139-145.

[34] M.R. Samarghandi, M. Siboni, A. Maleki, S.J. Jafari, F. Nazemi, J. Mazandaran Univ. Med. Sci. 21 (2011) 44-52.

[35] E. Bazrafshan, F. Kord Mostafapour, B. Barikbin, J. Birjand Univ. Med. Sci. 19 (2012) 266-276.

[36] M. EL. Alouani, S. Alehyen, M. EL. Achouri, M. Taibi. J. Mater. Environ. Sci. 9 (2018)32-46.

[37] H. Ayoub, M. Kassir, M. Raad, H. Bazzi, A. Hijazi. J. Mater. Civ. Eng. 5 (2017)31-45.

[38] A. Nezamzadeh-Ejhieh, M. Khorsandi, J. Hazard. Mater. 176 (2010) 629–637.

[39] H. Nassehinia, M. Gholami, A. Jonidi Jafari, A. Esrafili, Asian J. Chem. 25 (2013) 3427-3430.

[40] R.M. Mohamed, D.L. McKinney, W.M. Sigmund, Mater. Sci. Eng. 73 (2012) 1-13.

[41] A. Nezamzadeh-Ejhieh, Z. Ghanbari-Mobarakeh, J. Ind. Eng. Chem. 21 (2015) 668–676.